

## Analysis of Donor and Compensation Ratio in I-doped ZnSe by Far-Infrared Magneto-Absorption

*NTT Basic Research Laboratories, 3-9-11, Midori-cho, Musashino-shi Tokyo 180*  
Ken Saito and Syoji Yamada  
*NTT Opto-electronics Laboratories, Tokai-mura, Naka-gun, Ibaraki 319-11 Japan*  
Akira Ohki and Koshi Ando

### Abstract

The first far-infrared (FIR) magneto-absorption study is described of the shallow donors and compensation ratios of I-doped ZnSe. FIR experiments are carried out by observing Zeeman absorption spectroscopy using a FIR-laser with a high-magnetic field. From detailed analysis of the results, four different donor species are resolved and exact donor(I)-ionization energy is estimated. Also compensation ratios and absolute donor(acceptor) densities are determined.

### §1. Introduction

ZnSe has been investigated by many researchers, since it has the possibility of being utilized as blue-light emitting devices. Currently, the most important problem is conduction-type control, especially to obtain a stable p-type material. In this sense, it is of specific importance to know the impurity states and the compensation mechanism of ZnSe. Donor states (and acceptors) have so far been studied mainly by photoluminescence measurement<sup>1-3)</sup> and a binding energy of about 26 meV has been estimated. In addition, donor identification of Al, Cl, Ga, In, F and I has also been reported.<sup>4,5)</sup> However, there are few reports concerning the compensation ratio of ZnSe. On the other hand, FIR analysis for II-VI materials has been restricted so far to CdTe and CdSe,<sup>6)</sup> except for the recent cyclotron resonance measurement for ZnSe<sup>7)</sup> which primarily discussed free electron effective mass.

In this paper, the results of the first analysis of the shallow donors and compensation ratios of I(Iodine)-doped ZnSe by FIR magneto-absorption are described. This method has been successfully applied to GaAs<sup>8-10)</sup> and InP<sup>11)</sup> and was found to be a powerful tool to study shallow donor impurity and such related quantities as compensation ratio. Such a quantitative analysis can thus be a first-step towards clarifying the compensation mechanism of ZnSe.

### §2. Samples and FIR experiments

I-doped n-type ZnSe films with  $(N_d - N_a)$  of  $10^{15} \sim 10^{16}$  ( $\text{cm}^{-3}$ ) were used in this study. Parameter of used samples are listed in Table 1. Here  $N_d$  and  $N_a$  are total donor and acceptor density, respectively. All the samples were grown on semi-insulating GaAs(100) substrate by metalorganic vapor phase epitaxy.<sup>12)</sup> The FIR wavelength used was 57  $\mu\text{m}$  obtained from  $\text{CH}_3\text{OD}$  gas pumped by a  $\text{CO}_2$  laser. The sample was set in a superconductive magnet immersed in liquid He. Detection of the transmitted FIR power was carried out using a tunable Putley-type<sup>13)</sup> InSb detector. The donor species were resolved from each other by chemical shift in the  $1s-2p_{+1}$  absorption. To identify the donor species, secondary ion mass spectrometry (SIMS) analysis was also carried out. The resolved donors were separately calibrated by a Lorentzian curve fitting. A compensation ratio  $\theta = N_a/N_d$  was determined from absorp-

Table 1. Measured I-Doped ZnSe samples.

No.	$N_d - N_a$ ( $\text{cm}^{-3}$ )	Mobility <sub>300K</sub> ( $\text{cm}^2 \cdot \text{V}^{-1} \cdot \text{Sec}^{-1}$ )	Thickness ( $\mu\text{m}$ )
Z4	$5.0 \times 10^{15}$	320	3.5
Z8	$6.0 \times 10^{15}$	280	3.0
Z3	$1.0 \times 10^{16}$	280	4.5
Z7	$2.0 \times 10^{16}$	220	3.5
Z6	$7.0 \times 10^{16}$	200	2.0

tions taken under visible photoexcitation.<sup>10,14)</sup> The donor and acceptor densities were finally estimated in combination with the Hall measurement results at 300 K.

### §3. Results and Discussions

#### 3.1 Donor impurity and Ionization energy

We started the fundamental nature of the Zeeman spectra and the problem of donor impurity resolution. The Zeeman absorptions taken under photoexcitation for various I-doped samples are shown in figure 1. As shown in the figure, as much as four peaks are observed in the spectrum of sample Z4, which has the lowest ( $N_d - N_a$ ) concentration. These peaks can be specified as indicated in the figure by comparison with hydrogenic model calculations.<sup>15)</sup> When ( $N_d - N_a$ ) increases, transitions to higher levels begin to vanish. Finally, no peaks are observed in sample Z6, which has the highest ( $N_d - N_a$ ). These results suggest that the hydrogenic model can be applied to donors in ZnSe with a low ( $N_d - N_a$ ). However, it cannot be applied to high ( $N_d - N_a$ ) samples,<sup>10)</sup> since impurity band nature plays a dominant role. This dependency suggests that the  $1s-2p_{+1}$  peak is suitable for shallow impurity analysis, which is very similar to the III-V material case.

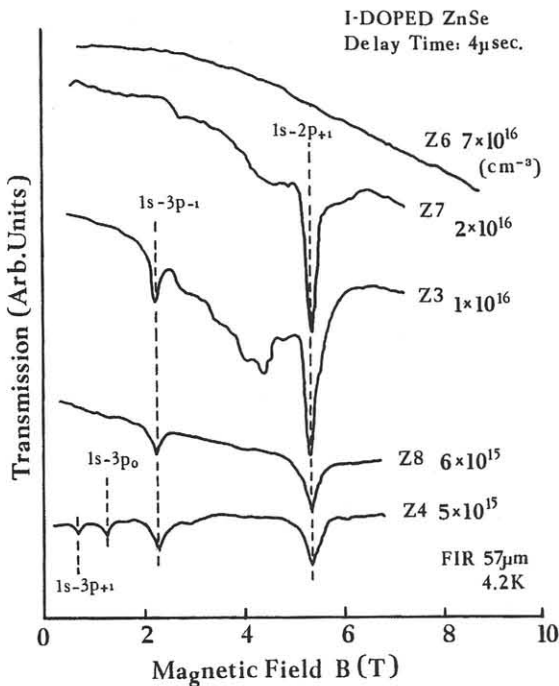


Fig. 1. Wide range Zeeman absorption spectra for various I-doped ZnSe for a FIR wavelength of 57  $\mu\text{m}$ . Higher transitions vanishing with increasing ( $N_d - N_a$ ) is due to the impurity band nature.

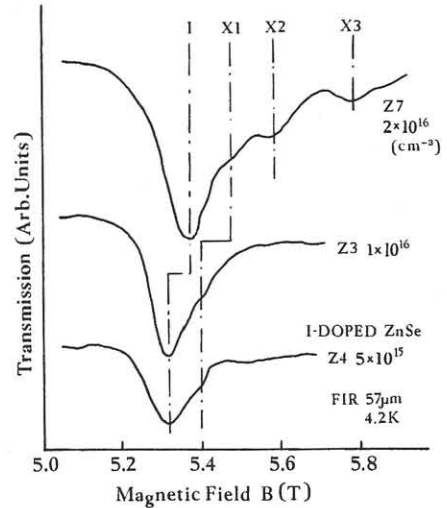


Fig. 2.  $1s-2p_{+1}$  peaks shown in extended scale. Fine structures corresponding to several donor impurities are clearly seen.

$1s-2p_{+1}$  peaks measured under a slow sweep condition are shown in figure 2. These peaks can be resolved into two subpeaks for Z3 and Z4, and four Z7, each of which most likely corresponds to a different impurity. The major subpeaks in most of the low field can be specified as Iodine, since only this species was detected in SIMS analysis. Moreover, the absorption intensity of the subpeaks is almost proportional to the I-doping concentration. Residual subpeaks X1~X3 cannot be identified at present. Iodine donor ionization energy is obtained by fitting the hydrogenic model calculation to the peak field value. This yields  $E_i=25.6$  meV, which is slightly smaller than the calculated  $E_i=26.06$  meV<sup>3)</sup> or reported value  $E_i=30.4$  meV.<sup>5)</sup> The former is obtained by assuming an electron effective mass of  $m_e^*/m_0=0.16$  and a permittivity ratio of  $\epsilon_r=9.14$ . The difference is likely due to the chemical shift of the Iodine first verified during this experiment.

#### 3.2 Compensation ratio and Impurity density

The absorption spectra of sample Z4 shown in figure 3 indicates the effect of visible photoexcitation. In this figure, the vertical scale, *transmission*, is a logarithm of the transmitted FIR power. The area of the absorption signal is then considered as the absorption cross section for each case. If the proper delay time,  $\tau_d$ , is selected, the ratio of signal area between (1) and (3) in Fig. 3, yielding a compensation ratio  $\theta = N_a/N_d$ . Here,  $\tau_d$  is the delay time after visible photoexcitation. In this experiment, the relaxation process of the photoexcited electrons is

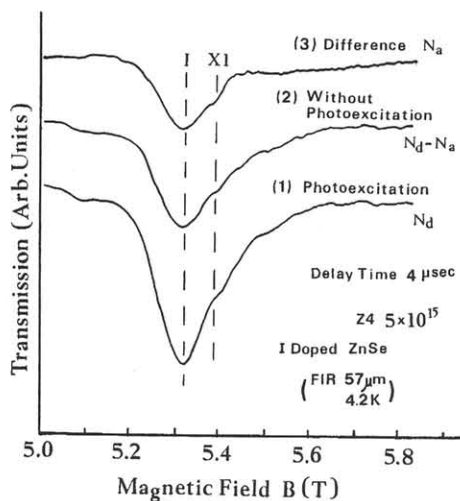


Fig. 3. Variations in  $1s-2p_{+1}$  transition under visible photoexcitation. Absorption areas of each waveform, (1), (2) and (3), represent quantities of  $N_d$ ,  $(N_d - N_a)$  and  $N_a$ , respectively.

important and in this sense, delay time  $\tau_d$  is a key parameter. The dependency of  $\theta$  and the absorption intensities on delay time  $\tau_d$  are shown in Fig. 4 for the sample Z3. Here, the  $\theta$  remains constant when  $\tau_d$  is shorter than about  $10 \mu\text{sec}$ . Within that time, almost of all the donors are neutralized by the excited electrons. If the delay time is shorter than  $10 \mu\text{sec}$ ,  $\theta$  can be accurately determined.

If the compensation ratio  $\theta$  is known, values of  $N_d$  and  $N_a$  are easily obtained in combination with the results of the Hall measurement and are listed in Table 1. The quantities  $N_d$ ,  $N_a$  and  $\theta$  determined for various samples are summarized in Table 2 and SIMS results in terms of the  $I/\text{Se}_{-3}$  ratio are also listed. Finally, the quantity of each resolved donor impurity

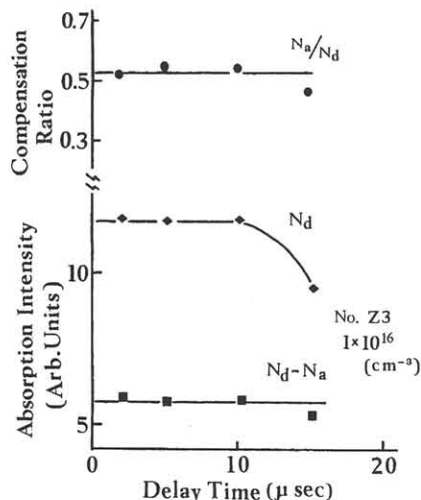


Fig. 4. Dependency of compensation ratio and absorption intensities upon delay time  $\tau_d$ . Proper  $\tau_d$  is selected using these results.

Table 2. Results of FIR Magneto-Absorption Analysis.

No.	FIR			SIMS
	$N_a/N_d$ ( $\theta$ )	$N_d(I)$ ( $10^{16}\text{cm}^{-3}$ )	$N_a$ ( $10^{16}\text{cm}^{-3}$ )	$I/\text{Se}_{-3}$
Z4	0.33	0.76	0.26	$1.3 \times 10^{-3}$
Z8	0.28	0.83	0.23	
Z3	0.54	2.2	1.2	$1.9 \times 10^{-3}$
Z7	0.45	3.6	1.6	
Z6	not detected			$2.6 \times 10^{-2}$

can be estimated from the absorption spectra. The curve-fitting example for the samples Z4 and Z7 are shown in figure 5. As seen in the figure, the  $1s-2p_{+1}$  peaks are resolved into two and four components for Z4 and Z7, respectively. From this analysis, all residual impurities are found to be less than one fourth the quantity of the Iodine-donor doped intentionally.

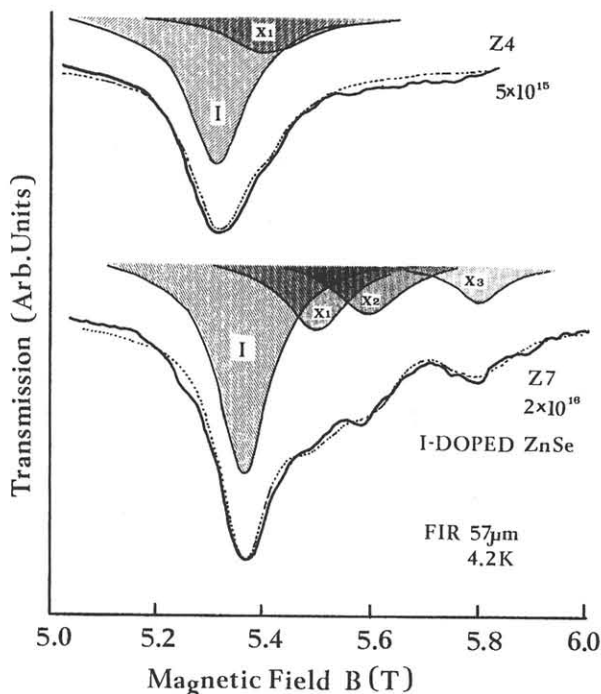


Fig. 5. Examples of Lorentzian curve-fitting to resolve and calibrate the individual donors incorporated. Thick solid lines are experimental. Dotted lines are fitted curves. Thin solid lines indicate resolved subpeaks.

### 3.3 Origin of acceptor and Compensation mechanism

From the results in the last subsection, we can plot the relation between absolute acceptor and donor concentrations as shown in Fig. 6. In the figure,  $N_a$  become negligibly small at about  $N_d = 6 \times 10^{15} \text{ (cm}^{-3}\text{)}$  and linearly increases to a logarithm of  $N_d$ . This result indicates that there is some relationship

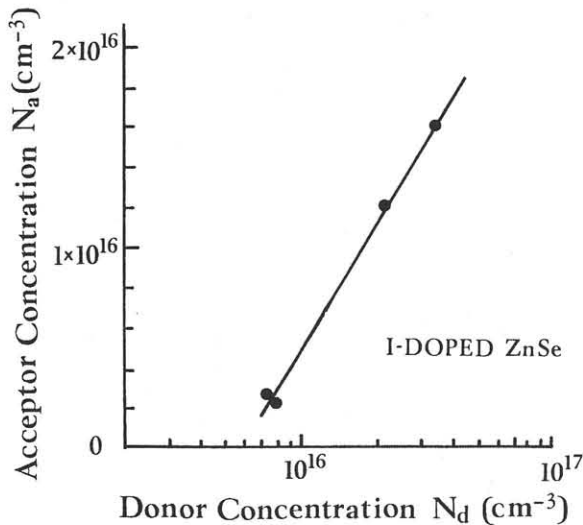


Fig. 6. Acceptor density plotted as a function of Iodine donor density. The former is almost zero at  $N_d \sim 6 \times 10^{15}$  ( $\text{cm}^{-3}$ ) and increases proportional to the logarithm of  $N_d$ .

between the two quantities. In other words,  $N_a$  is likely to increase as I-doping increases above a certain critical value. One possible explanation for the observed relation is that if dopant I increases, some sort of lattice defects, Zn-vacancy or the complex might be induced as compensating acceptor centers. This assumption seems realistic when the following two facts are taken into account. One is that no SIMS signal corresponds to the acceptor impurities suggesting, that they are below the usual SIMS detection limit of  $\sim 1 \times 10^{16}$  ( $\text{cm}^{-3}$ ), even though the acceptor density of samples Z3 and Z7 are sufficiently large. The other fact is that D-A pair transition has not been observed in photoluminescence measurement of the I-doped samples. These facts also suggest that the acceptors in I-doped ZnSe are not simple shallow acceptor, but deep ones.

Another explanation is that the compensating acceptors are efficiently coupled to donor state, forming dipole-type pair center.<sup>16)</sup> This donor-acceptor pairing might cause the reduction in donor ionization energy and also play as inactive scattering center for carrier transport. Details are not fully understood this at stage, but such acceptor and Iodine donor might both dominated the compensation mechanism in the studied ZnSe films.

#### §4. Conclusion

In summary, the donors and compensation ratios

of I-doped epitaxial ZnSe were estimated by the FIR absorption method. Besides the Iodine donor, three residuals were found to be included in the samples. The compensation ratio was at most about 0.5 when  $(N_d - N_a) \sim 1 \times 10^{16}$  ( $\text{cm}^{-3}$ ). It was found that acceptor density increases with increases in the Iodine dopant, even though a negligible amount of acceptor impurities was found during the SIMS analysis. Two possible models for compensating acceptor state (deep complex or pair state coupled to donor) are presented. The work is continuing to further elucidate compensation mechanism in n- and p-type ZnSe.

#### Acknowledgement

The authors wish to express their gratitude for the guidance of Dr. Yoshiji Horikoshi, Dr. Kei Murase, Dr. Kiyomasa Sugii, and Dr. Akinori Katsui.

#### References

- 1) R. N. Bhargava, R. J. Seymour, B. J. Fitzpatrick and S. P. Herk: *Phys.Rev.B*, **20**, 6, 2407(1979).
- 2) P. J. Dean, S. Stutius, G. F. Neumark, B. J. Fitzpatrick and R. N. Bhargava: *Phys.Rev. B*, **27**, 4, 2419(1983).
- 3) M. Isshiki: *J.Cryst.Growth*, **86**, 615(1988).
- 4) J. L. Merz, H. Kukimoto, K. Nassau and J. W. Schiever: *Phys.Rev.B*, **16**, 6, 545(1972).
- 5) P. Blanconnier, J. F. Hogrel, A. M. Jean-Louis and B. Sermage: *J.Appl.Phys.*, **52**, 11, 6895(1981).
- 6) P. E. Simmonds, J. M. Chamberlain, R. A. Hoult, R. A. Stradling and C. C. Bradley: *J.Phys.C:Solid State Phys.*, **7**, 4164(1974).
- 7) T. Ohyama, K. Sakakibara and E. Otsuka, M. Isshiki and K. Igaki: *Phys.Rev.B*, **37**, 11, 6153(1988).
- 8) G. E. Stillman, C. W. Wolfe and J. O. Dimmock: *Semicon. & Semimetals*, Vol.12, Chapt.4, 169, edited by K.J.Button(Academic Press, New York, 1977).
- 9) T. Ohyama and E. Otsuka: *Infrared and millimeter Waves*, Vol. 8, Chap.6, 214, edited by K. J. Button(Academic Press, New York, 1983).
- 10) K. Saito and S. Yamada: *Jpn J.Appl.Phys.*, **29**, L194(1990).
- 11) S. Yamada, K. Uwai, Y. Kawaguchi, E. Kubota and S. Kondo: 4th.Int.Conf.Semiconducting III-V materials, Hakone, 207(North-Holl and Amsterdam, 1986).
- 12) N. Shibata, A. Ohki and A. Katsui: *J.Cryst.Growth*, **93**, 703(1988).
- 13) E. H. Putley: *Proc.IEEE.*, **11**, 1412(1963)
- 14) B. O. Kolbesen: *Appl.Phys.Lett.*, **27**, 353(1975).
- 15) S. Narita and M. Miyao: *Solid State Comm.*, **9**, 2161(1971).
- 16) T. Yao: *J.Cryst.Growth*, **72**, 31, (1985)